ASPS Conference Proceedings 1: 491-497 (2022)

Proceedings of

12th Structural Engineering Convention - An International Event (SEC 2022)

Available at https://asps-journals.com/index.php/acp

Nonlinear Seismic Analysis of Perforated cold-formed steel shear wall with Upright Section

Simran Senapati [1, *], Keshav K. Sangle [2]

[1] Department of Structural Engineering, Veermata Jijabai Technological Institute, Research Scholar, Mumbai, 400019, India
[2] Department of Structural Engineering, Veermata Jijabai Technological Institute, Professor, Mumbai, 400019, India

Paper ID - 040491

Abstract

During the last few decades, cold-formed steel (CFS) is extensively used in mid- and low-rise housing due to the increasing demand of rapid constructions along with its various advantages in comparison with other structural material. Cold-formed steel framed shear walls (CFSFSW) are most common and primary lateral load resisting system. However, adopting it in the seismic zone is difficult, especially because many design components remain open. In this research an effort has been made to design the shear wall system with both unperforated and perforated upright sections using nonlinear static analysis method. In ABAQUS, a general-purpose finite element analysis software, three-dimensional models using shell elements are used to simulate a shear wall system. A comparative study regarding the lateral load capacities with respect to maximum allowable lateral deflection including different parameters like column sections, thickness and perforation arrangements are presented here. It was found that increasing thickness and including Chanel stiffeners improves the lateral strength of original upright section. The developed modelling protocol helps to estimate its lateral performance under earthquake with reasonable accuracy.

Keywords: Cold-formed steel, ABAQUS, Nonlinear analysis, Shear wall, Lateral load, Upright Section, Perforation

1. Introduction

Over the last four decades, there has been an increasing trend to use CFS sections as principal structural components in construction of low to medium-rise houses, multi-story commercial structures, and modest-span portal frames.[1][2] It is becoming increasingly popular because of it's ability to meet the demand for low-cost and high-performance structures. The flexibility given by the huge variety of shapes, section measurements, short execution time, lightweight arrangements and the high quality of the end products, are only a few of the advantages. The principal structural elements, such as columns, beams, and roof truss members[2], are made from CFS which are often used as load-bearing components in lightweight structures and pre-fabricated constructions[3]. CFSFSW are used as primary lateral load resisting system utilized in seismic areas owing to their minimal maintenance, ease of transport, handling, and high strength-to-weight ratio over time also improved building performance and structural function. There have been lot of research done in CFS framing resisting systems with different sheathing materials[4] and studies have been done to investigate the flexural behavior for calculation of lateral load capacity of CFS members. Study involving Finite Element Analysis (FEA) to investigate the flexural strength of built-up sections and parametric studies were performed earlier and have given promising results[5]. In addition to regular channel section, experimental and FEM investigation were also carried out for unequal angle sections [6] as well as upright column sections[7] and their performance have been duly validated. On CFS members with perforation(holes), much research has been conducted. An analysis of rectangular holes in a lipped channel section revealed that location of holes in relation to effective area provides a precise design strategy [8]. Nonlinear finite element modelling techniques were developed based on experimental investigation regarding effect of holes on elastic buckling [9] and ultimate strength[10]. A limited number of studies had reported the influence of perforations on the structural behaviour of upright columns ,which were mostly used for storage racks [11][12]. Sangle et al. investigated the three dimensional model of traditional pallet racking system and presented the stability analysis [13] ,which experimental results were further validated by Thombare et al. [14] using ABAQUS . It was found that the analytical results of FE models were in good agreement with experimental results. The focus of this paper lies in extending the research for the design of CFSFSW with both un-perforated and perforated sections used as column section and estimating its lateral performance under earthquake.

*Corresponding author. Tel: +9124198141; E-mail address: sksenapati_p18@ci.vjti.ac.in

Published online: December 19, 2022
doi:10.38208/acp.v1.539

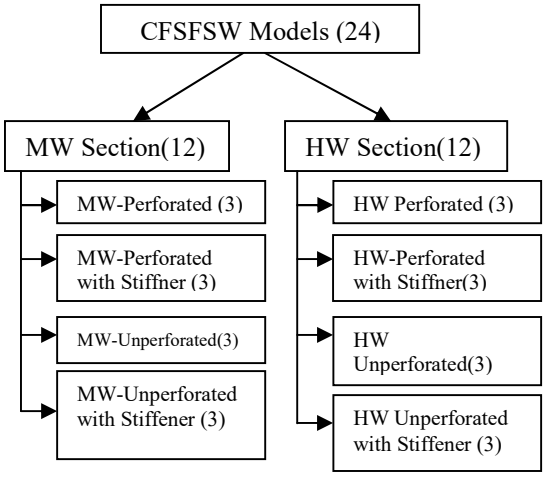

Fig 1. Details of CFSFSW Models

The CFS frames consist of column-sections, upper track and lower track members. Due to the relationship between steel pieces and their connections, seismic performance of the CFSFSW is one of the challenges in design. Steel frame members subjected to advanced numerical modelling and nonlinear analysis using linear, hybrid-linear and shell components have received a lot of attention in recent days.

Brief research outline of this paper is to learn more about overall response of lateral loads and to develop FEM model of CFSFSW with upright column sections , MW (Medium Weight) and HW(Heavy Weight) along with channel as external stiffeners using FE software ABAQUS [15]. Primary and final purpose of this research is to give design guidelines for these systems based on a finite element modelling overview. This research also aims to improve CFS building capabilities while delivering essential performance requirements for final application of design codes.

2. Modelling Approaches

Models implemented in this paper are CFSFSW under lateral load developed using ABAQUS/Standard Version 6.14.1 [16] . In total 24 models have been developed based on up-right section i.e. 12 models have been modelled using MW section and 12 models using HW section which is further divided based on perforation and inclusion of channel stiffener as detailed in Fig 1.
The simulated shear wall consists of upright CFS columns, intermediate stud, tracks and channel sections as external stiffeners as shown in Figs. 3. (a)-(d). The column sections are perforated to facilitate the beam end connector installation easier. Geometric nonlinearities are included in the analysis using the Newton-Raphson approach, which is the default nonlinear solution in ABAQUS.

3. Test Specimen

3.1. Model Geometry:

The 24 CFSFSW models used in this study have width of 1200 mm and a height of 2400 mm. As illustrated in Figs. 2. (a)-(b), the column sections included in this model are MW sections with various thicknesses (1.6 mm, 1.8 mm, and 2.0 mm) and HW sections with thicknesses of 2.0 mm, 2.25 mm, and 2.5 mm. These cross-sectional geometry and perforation details have taken from [13] and the node data used for modelling are mention in Table II. All material properties of both sections have been tabulated in Table III.
Un-lipped channel sections have been used for track members and mid-width intermediate stud in this CFS frame. The thickness for track, intermediate stud and channel stiffener have 1.2 mm. Table I displays the dimension of CFS members implemented in this paper.

All elements have been assembled together as shown in Fig 4.

TABLE I: Dimension of CFS members

CFS Members In Model	For MW Upright section	For HW Upright Section
	(All dimensions are in mm)	
Track Member	31.2×76.4×1200	32×104×1200
Intermediate stud	31.2×76.4×2400	32×104×2400
Channel stiffener	20.7×31.6×2400	31×58×2400

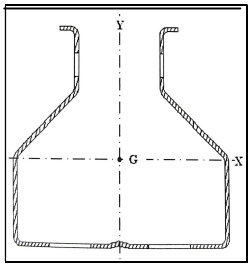

Fig 2. (a) MW section

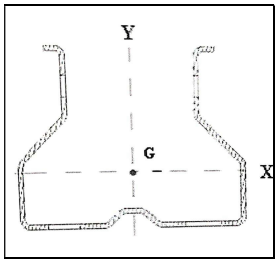

Fig 2. (b) HW section

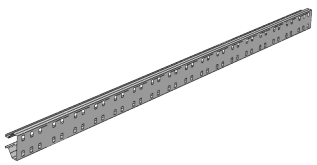

a) Stud

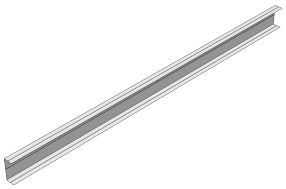

b)Track

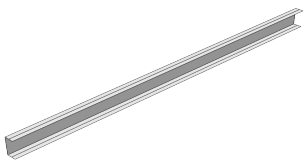

c)Intermediate stud

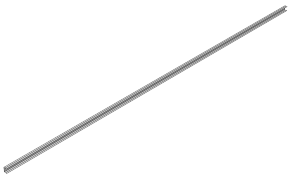

d) channel stiffener

Fig. 3. a) stud, b) track and c) Intermediate stud d) channel stiffener

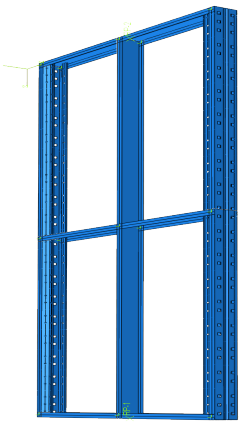

Fig. 4. Perforated CFSFSW

TABLE II: NODE DATA OF BOTH MW AND HW SECTION

MW SECTION		HW SECTION	
X COORD	Y COORD	X COORD	Y COORD
21.5	0	36	0
15.8	0	29	0
15.8	-7.25	29	-11.55
15.8	-15.75	29	-22.05
15.8	-20.7	29	-31
38.2	-45.2	52	-54
38.2	-76.4	52	-86
25.5	-76.4	39	-86
10.5	-76.4	23.5	-86
-10.5	-76.4	11	-86
-25.5	-76.4	4	-80
-38.2	-76.4	-4	-80
-38.2	-45.2	-11	-86
-15.8	-20.7	-23.5	-86
-15.8	-15.75	-39	-86
-15.8	-7.25	-52	-86
-15.8	0	-52	-54
-21.5	0	-29	-31
		-29	-22.05
		-29	-11.55
		-29	0
		-36	0

3.2. Mesh Discretization

As mesh elements for members, 4 noded general purpose shell finite elements (S4R) are utilized. It has been observed that mesh density in CFS members greatly affects performance[17].Coarse mesh doesn't capture Local buckling modes but they do capture distortional and global buckling modes. In contrast, a finer mesh accurately reflects all types of buckling modes. Additionally, when an appropriate mesh is adopted, the difference in reaction between different kinds of elements is minimised. In this modelling attempt, a fine mesh is used for these purposes, as seen in Figs. 5(a)-(b). From convergence study [14] a mesh size of 10mm x 10mm is found to be suitable for present work CFS members and has been incorporated in the model.

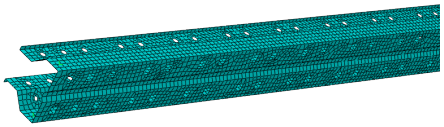

a) stud

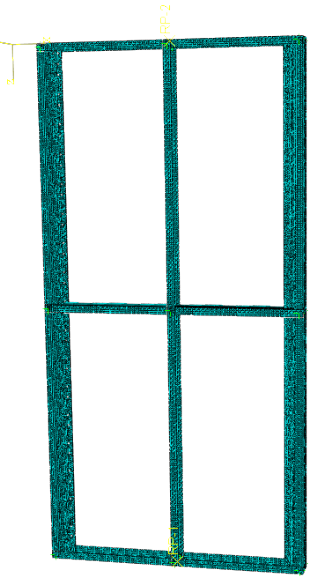

b) CFS shear wall frame

Fig. 5 Shell finite element mesh formation of a) stud b) CFS Shear wall frame

3.3. Material Properties

CFS model used in this study is isotropic and plastic, having Young's modulus of E= 212000 N/mm2 and Poisson's ratio(μ) of 0.29 details as tabulate in Table-III. In the computational modelling of CFS, this value for Young's modulus E is widely used. This sort of material is permissible, according to the ABAQUS analysis user's guide. For nonlinear static analysis (plastic) Isotropic hardening of CFS members was adopted [18] as shown in Table-IV.

TABLE III: Material Properties used for CFS-Modeling

Material Properties	Value
E (Young's Modulus)	212000 N/mm ^{2}
μ (Poisson's ratio)	0.29
ρ (Mass density)	7860 kg/m^3

TABLE IV: Material stress-strain Properties

Yield Stress (N/mm^2)	Plastic Strain
401.96	0
413.69	0.005
424.72	0.01
441.26	0.015
484.01	0.025
512.97	0.035
534.34	0.045
551.58	0.055
564.68	0.065
575.71	0.075
585.36	0.085
593.63	0.095
601.22	0.105

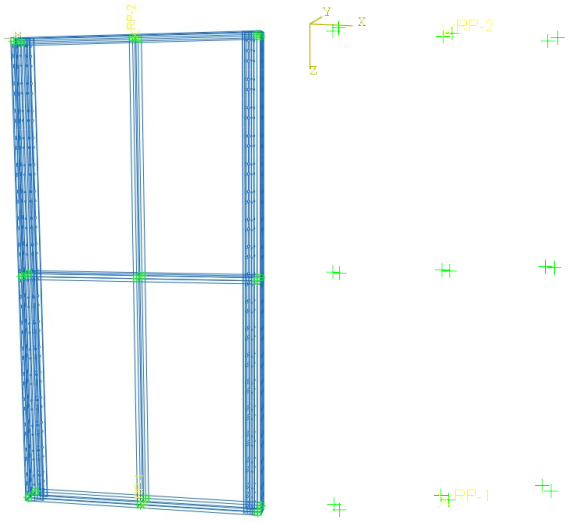

Fig.6 a) CFS-CFS_ connection Fig.6(b) Screw Model
Fig.6 Connection Detailing

3.4. Fastener connection

CFS sections are modelled using a mesh independent fastener technique. Developing a point-to-point link between distinct surfaces is simple with mesh-independent fasteners. Each layer uses a connector function to link two fastening points. The model includes one connector section: screw for interaction between steel members on the open side (Hex washer) of diameter 4.78 mm from ABAQUS library as manifested in Figs. 6(a-b).

3.5. Boundary Condition and Loading

The bottom track is restrained by using fixed nodes as shown in Fig 7 (a). The top track is restrained by restraining the out of plane displacement as shown in Fig 7 (b). By using a displacement control of 0.127 mm, the top track of the CFSFSW has been subjected to lateral-monotonic load (Liu 2014)[19]. As shown in Fig. 7, the RIGID_BODY command in Abaqus is used to join one end of cross-section in top track to a reference node at its centroid.

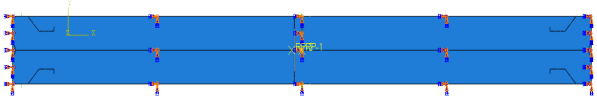

Fig 7 (a) Bottom Track Boundary condition

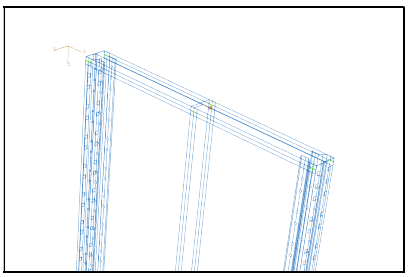

Fig 7 (b) Top Track loading condition

Fig.7. Loading Model

4. Finite Element Modelling

In ABAQUS, the modelling technique is utilized to develop a set of 24 shell finite element models with high precision and the computed results of this model analysis are compared to a variety of parameters such as column section, thickness, channel stiffener, and perforation. The force-displacement behavior, and lateral load capacity for maximum allowable lateral deflection, which is 9.6mm (0.004 times the height of the frame) as per IS 1893:2016 for each model are presented in the paper.

4.1. Force-Displacement Behavior Analysis

The force- displacement behavior of the generated Abaqus models are shown in Figs. 8 (a)-(f). Table V summarises the computational results, including the lateral load P_e (kN) of the respective model for 9.6 mm lateral displacement.

TABLE V: Computational result

Model	Thickness (mm)	P_e (kN) for 9.6 mm Δ
MW-1.6-U1	1.6	14.39
MW-1.8-U1	1.8	15.30
MW-2.0-U1	2.0	16.13
HW-2.0-U1	2.0	18.02
HW-2.25-U1	2.25	18.15
HW-2.50-U1	2.50	18.23
MCW-1.6-U1	1.6	14.84
MCW-1.8-U1	1.8	15.67
MCW-2.0-U1	2.0	16.57
HCW-2.0-U1	2.0	18.21
HCW-2.25-U1	2.25	18.28
HCW-2.50-U1	2.50	18.35
MW-1.6-P1	1.6	13.99
MW-1.8-P1	1.8	14.92
MW-2.0-P1	2.0	15.73
HW-2.0-P1	2.0	17.73
HW-2.25-P1	2.25	18.13
HW-2.50-P1	2.50	18.20
MCW-1.6-P1	1.6	15.60
MCW-1.8-P1	1.8	16.41
MCW-2.0-P1	2.0	17.14
HCW-2.0-P1	2.0	18.21
HCW-2.25-P1	2.25	18.23
HCW-2.50-P1	2.50	18.31

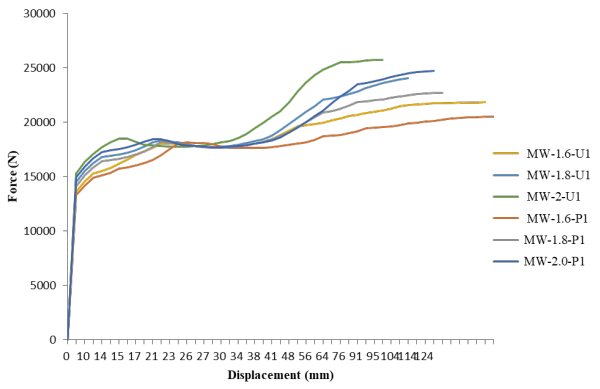

Fig. 8.a) MW Section with varying thickness

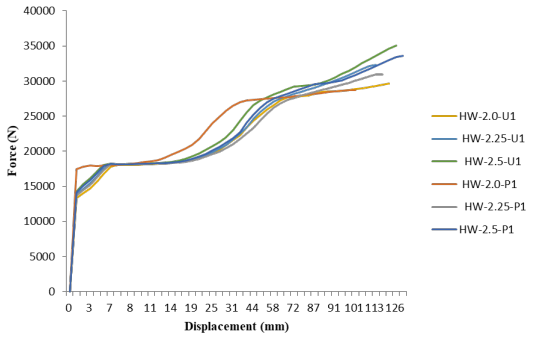

Fig. 8.b) HW Section with varying thickness

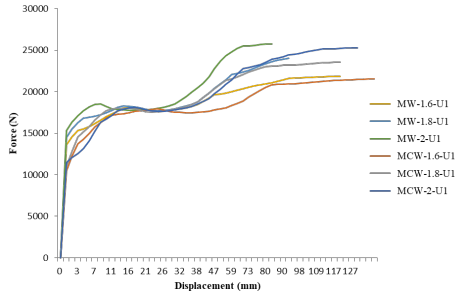

Fig. 8.c) MW section with and without stiffener(unperforated)

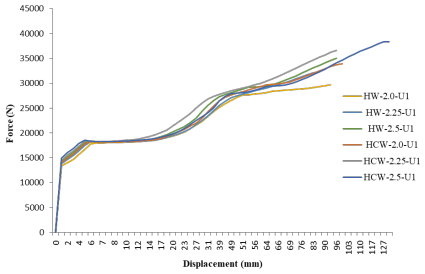

Fig. 8.d) HW section with and without stiffener (unperforated)

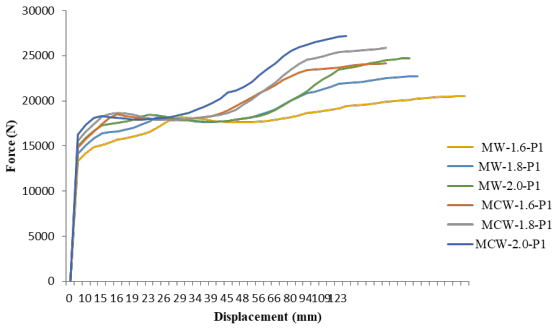

Fig. 8.e) MW section with and without stiffener(perforated)

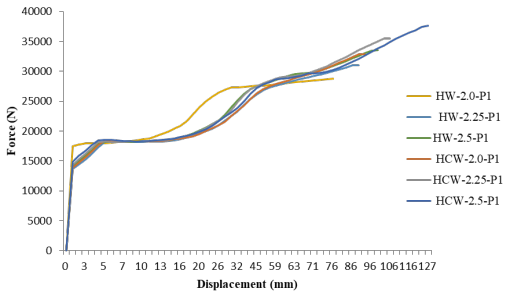

Fig. 8.f) HW section with and without stiffener(perforated)

Fig.8. Force vs. Displacement curve

4.2. Stud to Track Connection Failure

The proposed FE models can be used to examine how shear force is transferred to the fasteners in the shear wall. Figure 9 depicts the deformed shape of Model MW-2.0-P1 at the conclusion of the analysis, with a focus on the stud-to-track fasteners. Because of the symmetry, stress concentration due to connection on bottom track and left side of the shear-wall are not shown in this figure. It is observed that the stress concentration near the connection of stud and track reaches it's maximum value when it attains the peak load.

4.3. Deformation Study of CFSFSW:

Some of the advantages of the Abaqus computational models used in this study are their ability to grasp most of the buckling modes and graphical representation of the deformed shape with stress allocation in the shear walls. Specifically, for Model MW-2.0-P1, Fig. 10 shows the deformed shape of the CFSFSW. Contour values are represented by colours varying from red (maximum value) to blue (minimum value). When the model is subjected to a complex loading condition, Von Mises stress is usually employed to determine if it yields. The Fig. 9 reveal a high concentration of stress on track flanges at the connection between stud-to-track.

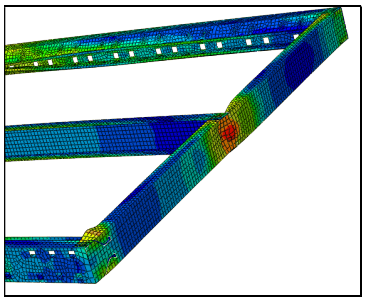

Fig.9 Track to Stud Connection Failure

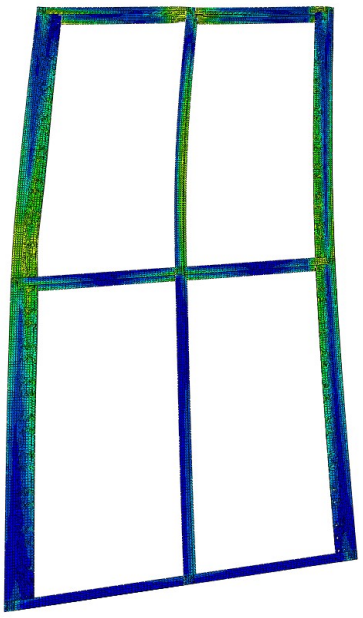

Fig.10 Deformed shape of MW-2.0-P1

5. Conclusions and Discussion

CFSFSW computational modelling is developed, with Abaqus. The designed modelling approach was shown to be capable of accurately capturing lateral load bearing capacity.

The graphs of Load vs. deflection for CFSFSW with and without perforation of various thicknesses are plotted. Following observations regarding lateral load capacities (LLC) were found for different section varying the thickness.

i. MW section (unperforated) with thickness of 1.8 mm and of 2 mm are more than 6.32 % and 12.09 % as compared to thickness 1.6 mm.
ii. HW section (unperforated) with thickness of 2.25 mm and 2.5 mm are about 0.72 % and 1.17 % more than that of with thickness 2.0 mm.
iii. MW section (perforated) with thickness of 1.8 mm and 2.0 mm are 6.65 % and 12.44 % more than that of with thickness 1.6 mm.
iv. HW section (perforated) with thickness of 2.25 mm and 2.5 mm are more than 2.26 % and 2.65 % than with thickness 2.0 mm.

From this we can conclude that increasing thickness improves the lateral load carrying capacity as shown in graph 8 (a)-(b).

Following comparative observations regarding lateral load capacities were found for section with and without perforations.

i. MW section (perforated) having thickness 1.6 mm ,1.8 mm and 2 mm is less than 2.78%, 2.48 % and 2.48 % as compared to MW section (unperforated) with thickness 1.6 mm,1.8 mm and 2 mm respectively.
ii. HW section (perforated) having thickness 2 mm, 2.25 mm and 2.5 mm is 12.71 % ,0.11 % and 0.16 % less than that of due to HW Shear wall with thickness 2 mm, 2.25 mm and 2.5 mm respectively.

So, use of perforation decreases the lateral load carrying capacity as shown in graph 8 (a)- (b).

Following comparative observations regarding lateral load capacities were found for section with and without stiffeners.

i. MW Section (unperforated) with channel stiffeners having thicknesses 1.6 mm, 1.8 mm and 2 mm, is 3.13% ,2.12% and 2.73% more than MW shear wall(unperforated) without stiffeners having thicknesses 1.6 mm, 1.8 mm and 2 mm respectively.
ii. MW Section (perforated) with channel stiffeners having thicknesses 1.6 mm, 1.8 mm and 2 mm is 11.51% ,9.99% and 8.96% more than MW shear wall (perforated) without stiffeners having thicknesses 1.6 mm, 1.8 mm and 2 mm respectively.
iii. HW Section (unperforated) with channel stiffeners having thicknesses as 2 mm, 2.25 mm and 2.5 mm is 1.05 % ,0.72% and 0.66 % more than HW shear wall(unperforated) without stiffeners having thicknesses 2 mm, 2.25 mm and 2.5 mm respectively.
iv. HW Section (perforated) with channel stiffeners having thicknesses as 1.6 mm, 1.8 mm and 2 mm is 2.71% ,0.55% and 0.60% more than HW Section(perforated) without stiffeners having thicknesses 2 mm, 2.25 mm and 2.5 mm respectively.

So, it can be determined that channel stiffeners improve the lateral load carrying capacity for both MW and HW section as shown in Figs. 8 (c)- (f).

Both connection failure mechanisms and deformation of CFSFSW were discussed. It was observed that there was higher stress concentration near the connection between stud and track. So, we can use bracing members in the future to improve the result.

Disclosures

Free Access to this article is sponsored by SARL ALPHA CRISTO INDUSTRIAL.

References

[1] W. K. Yu, K. F. Chung, eta M. F. Wong, *„Analysis of bolted moment connections in cold-formed steel beam – column sub-frames*, libk. 61, or. 1332–1352, 2005.

[2] Y. H. Lee, C. S. Tan, S. Mohammad, M. Tahir, eta P. N. Shek, *„Review on Cold-Formed Steel Connections*, libk. 2014, 2014.

[3] Y. Li, M. Wang, G. Li, eta B. Jiang, *„Jo ur na l P of*, *Fire Saf. J.*, or. 103237, 2020.

[4] R. L. Madsen, T. A. Castle, eta B. W. Schafer, *„NEHRP Seismic Design Technical Brief No . 12 Seismic Design of Cold-Formed Steel Lateral Load-Resisting Systems A Guide for Practicing Engineers*, zenb. 12.

[5] L. Xu, P. Sultana, eta X. Zhou, *„Thin-Walled Structures Flexural strength of cold-formed steel built-up box sections*, libk. 47, or. 807–815, 2009.

[6] B. Young eta E. Ellobody, *„Design of cold-formed steel unequal angle compression members*, libk. 45, or. 330–338, 2007.

[7] K. M. Bajoria eta R. S. Talikoti, *„Determination of flexibility of beam-to-column connectors used in thin walled cold-formed steel pallet racking systems*, libk. 44, or. 372–380, 2006.

[8] O. Brookes, *„P REDICTION OF U LTIMATE C APACITY L IPPED C HANNELS OF*, zenb. May, or. 510–514, 1999.

[9] C. D. Moen eta B. W. Schafer, *„Scholars ' Mine Impact of Holes on the Elastic Buckling of Cold-formed Steel Columns*, 2006.

[10] C. D. M. Ã eta B. W. Schafer, *„Experiments on cold-*

formed steel columns with holes, libk. 46, or. 1164–1182, 2008.

[11] A. Crisan, V. Ungureanu, eta D. Dubina, ‚*Thin-Walled Structures Behaviour of cold-formed steel perforated sections in compression . Part 1 — Experimental investigations*, *Thin Walled Struct.*, libk. 61, or. 86–96, 2012.

[12] X. Zhao, C. Ren, eta R. Qin, ‚*Thin – Walled Structures*, libk. 112, zenb. November 2016, or. 2016–2018, 2017.

[13] E. Scholar, ‚*Stability and dynamic analysis of cold-formed storage rack structures with semirigid connections*, libk. 11, zenb. 6, 2011.

[14] C. N. Thombare, K. K. Sangle, V. M. Mohitkar, S. B. Kharmale, eta A. Mechanics, ‚*Nonlinear Static Pushover Analysis of Cold-Formed Steel Storage Rack Structures*, zenb. December 2015, or. 13–26, 2016.

[15] D. Systèmes, ‚*Volume IV: Elements*, *ABAQUS 6.14 Anal. User's Guid.*, libk. IV, 2014.

[16] S. P. Hibbitt D, Karlsson B, ‚*ABAQUS / CAE User ' s Manual*, *ABAQUS/CAE User's Man.*, libk. 1 and 2, or. 1–847, 2001.

[17] B. W. Schafer, Z. Li, eta C. D. Moen, ‚*Computational modeling of cold-formed steel*, *Thin-Walled Struct.*, libk. 48, zenb. 10–11, or. 752–762, 2010.

[18] C. D. Moen, ‚*Direct Strength Design of Cold-Formed Steel Members with Perforations*, zenb. August, 2008.

[19] P. Liu, K. D. Peterman, eta B. W. Schafer, ‚*Impact of construction details on OSB-sheathed cold-formed steel framed shear walls*, *J. Constr. Steel Res.*, libk. 101, or. 114–123, 2014.